Rheological and Resistance Properties of Magnetorheological Elastomer with Cobalt for Sensor Application

Afiq Azri Zainudin [1] **, Nurul Azhani Yunus** [2,*] **, Saiful Amri Mazlan** [1,3,*] **,**
Muhammad Kashfi Shabdin [3] **, Siti Aishah Abdul Aziz** [1,3] **, Nur Azmah Nordin** [1] **,**
Nurhazimah Nazmi [1] **and Mohd Azizi Abdul Rahman** [3]

[1] Engineering Materials and Structures (eMast) iKohza, Malaysia-Japan International Institute of Technology (MJIIT), Universiti Teknologi Malaysia, Jalan Sultan Yahya Petra, Kuala Lumpur 54100, Malaysia; afiqzn@gmail.com (A.A.Z.); aishah118@gmail.com (S.A.A.A.); nurazmah.nordin@utm.my (N.A.N.); nurhazimah@utm.my (N.N.)

[2] Department of Mechanical Engineering, Universiti Teknologi PETRONAS, Seri Iskandar 32610, Malaysia

[3] Advanced Vehicle System (AVS) Research Group, Universiti Teknologi Malaysia, Jalan Sultan Yahya Petra, Kuala Lumpur 54100, Malaysia; dekashaf@gmail.com (M.K.S.); azizi.kl@utm.my (M.A.A.R.)

* Correspondence: azhani.yunus@utp.edu.my (N.A.Y.); amri.kl@utm.my (S.A.M.)

check for updates

Abstract: Cobalt particles have been introduced as a filler due to the advantages of embedding their magnetic and electrical properties in magnetorheological elastomer (MRE). In the present research, the rheology and resistance of MRE are experimentally evaluated. Isotropic and anisotropic MRE samples containing silicone rubber and cobalt particles were fabricated. The magnetic properties of MRE are conducted using a vibrating sample magnetometer (VSM). The morphological aspects of MRE are observed by using field emission scanning electron microscopy (FESEM) and characterized by energy-dispersive X-ray spectroscopy (EDX). Rheological properties under various magnetic field strengths were measured for the magnetic field, strain amplitude, and frequency sweep test by using a parallel-plate rheometer. Subsequently, the resistance of MRE is tested under different applied forces and magnetic fields. The MRE storage modulus depicted an enhancement in field-dependent modulus across all the applied magnetic fields. The electrical resistance generated from the sample can be manipulated by external magnetic fields and mechanical loads. The conductivity of MRE is due to the existence of cobalt arrangements observed by FESEM. By introducing cobalt as filler and obtaining satisfactory results, the study might open new avenues for cobalt to be used as filler in MRE fabrication for future sensing applications.

Keywords: magnetorheological elastomer; cobalt; resistance properties; rheological properties

1. Introduction

Nowadays magnetorheological elastomer (MRE) has attracted much attention since, in addition to its magnetic and rheological properties, it presents uncommon electrical properties leading to various engineering applications, for example, vibration absorbers [1–3], electromagnetic waves absorbers [4], dampers [5,6], and sensors [7,8]. MREs are smart materials with properties that can be altogether changed in a controlled manner by outer stimuli, for example, magnetic field, electric–magnetic field, temperature, and pH [9,10]. The sensitivity to the magnetic field is provided by magnetic nano- or microparticles incorporated into the polymer [11,12]. In general, the ultimate properties of MREs are subject to the magnetic particle, elastomer matrix, external magnetic field strength, and dispersion of particles in the elastomer matrix.

Up to now, carbonyl iron particles (CIPs) have been commonly used as magnetic particles in MRE. The particles are dispersed in numerous types of rubber matrixes such as natural rubber or silicone rubber [13–15]. Although this kind of magnetic particles exhibit a high magnetic saturation of elements as well as high permeability and low remnant magnetization, the electrical property investigation is still lacking in the previous study, in which researchers chose to add another filler, which is graphite (Gr) [16]. The introduction of Gr powder has been proved to generate a new electrical conductivity property, while maintaining the existing rheological properties of MRE. Li et al. introduced a force sensor utilizing Gr powder in a magnetorheological elastomer (Gr-MRE); the effect of the magnetic field on the resistivity response of the fabricated samples was tested using an experimental setup that included mechanical parts, an electrical circuit, and an LED display unit. The results revealed that the prototype force sensor could be used to detect the external forces at the selected force ranges [17]. On the other hand, Tian et al. fabricated two types of Gr-MRE by varying the conditions between isotropic and anisotropic. This difference in particle structure contributed toward the increment in the initial storage and loss moduli under the anisotropic condition, which explains that charge transport plays a significant role in the dielectric polarization in the anisotropic composite material containing magnetic particles within the matrix [18]. In different circumstances, Schûmann et al. [19] analyzed an electroconductive MRE exhibiting highly complex resistive behavior. The author used CIPs, carbon black, and silicone as the main ingredients for the MRE fabrication. The results revealed that the resistance increased from 100 to 2300 kΩ and then dropped exponentially to 1200 kΩ at 1% and 3% strain, which was within the linear elasticity region. In a most recent study, Shabdin et al. [20] investigated the resistance properties of MRE by introducing Gr powder mixed with CIPs. The author used Gr particles in order to achieve a high electrical conductivity. However, the mixture of CIPs and Gr caused the composition to be saturated and thus restricted the author to add more Gr to the composition; otherwise, the samples would be too brittle and not reliable.

Nevertheless, several studies have introduced the cobalt as magnetic particles in MRE. Tong et al. [21] studied the effect of cobalt shape on improving the interfacial interaction of MRE based on a cobalt–silicon rubber matrix, which indicated good storage modulus and MR effect. In their study, an anisotropic MRE with two types of particle shape, namely flower-like and spherical shape, were fabricated and analyzed. The result showed that the flower-like shape cobalt particles exhibited a higher performance of storage modulus for the frequency sweep test as compared to the spherical shape. However, only rheological and magnetic properties were reported in the study.

To the best of our knowledge, no study has been conducted on the resistance properties of cobalt-based MRE, which detailed the resistance properties of the MRE toward the presence of external magnetic field; this area is still lacking and interesting to be investigated. This would include investigating the impacts of magnetic field strength on the cobalt-based MRE under strain amplitude, frequency, and current sweep of testing parameters. Therefore, in this study, investigation of the response of cobalt as magnetic particles toward the rheological and resistance properties for isotropic and anisotropic MRE was comprehensively examined.

2. Methodology

2.1. Raw Materials

Cobalt powder containing 99.8% trace metal basis with an average of 2 μm diameter was obtained from Sigma-Aldrich (San Luis, MO, USA) and used as the magnetic particles. Moreover, silicone rubber (SR) NS 625 A are utilized as a matrix in the MRE fabrication together with the curing agent NS 625 B, which were both purchased from Nippon Steel Co. (Toyko, Japan).

2.2. MRE Fabrication

A single MRE was prepared through a mixing process. First, 47 wt % of SR was mixed with 53 wt % of cobalt powder using a mechanical stirrer at 280 rpm until the mixture was visually

homogenous. Then, 2% of the curing agent from the total weight percent was added, and the mixture was continuously stirred for another 1 min. In order to produce an anisotropic structure, the curing process was performed in room temperature of 25 °C at 0.3 T (239.31 KA/m) with an orientation magnetic field along the thickness of the sample for about 2 h. By curing the mixture in the existence of a magnetic field, the interaction caused by the field between the particle encourages them to form chains or columns aligned along the field direction. Figure 1 and Table 1 show the schematic diagram and wt % of material used for preparation of isotropic and anisotropic MRE.
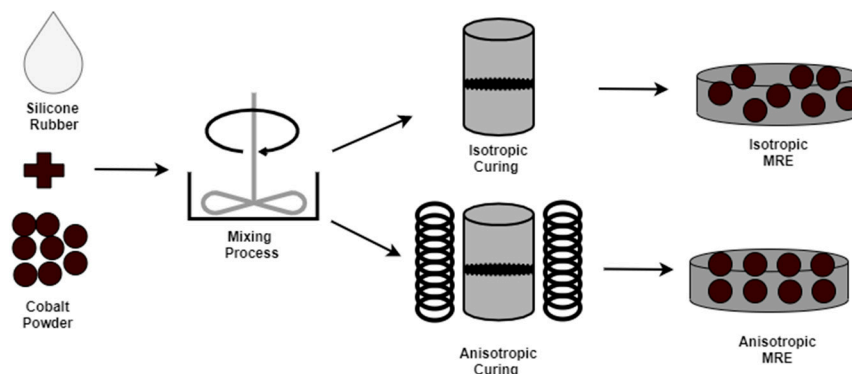

Figure 1. Schematic diagram of magnetorheological elastomer (MRE) preparation.

Table 1. Component of cobalt-based magnetorheological elastomer (MRE).

Compound Elements	Weight (g)	wt %
Silicon Rubber	4.7	47
Cobalt Powder	5.3	53

2.3. Material Characterization

The surface morphology of the MRE was examined using field emission scanning electron microscopy (FESEM): JSM-7800F PRIME, JEOL, Japan. The test was conducted with the application of an accelerating voltage of 6 kV with the magnification of 1000× and 3000× for the surface morphology. Therefore, energy-dispersive X-ray spectroscopy (EDX) was used to identify the elemental composition of MRE. The magnetic properties of the MRE were investigated using vibrating sample magnetometer (VSM); MicroSense, USA at room temperature. The sample weight of 0.08 g was mounted in the holder, which will vibrate during the analysis. Then, the test was subjected to a maximum magnetic field of 15,000 Oe.

2.4. Rheological and Resistance Properties

The rheological test was performed using a rotational rheometer (Physica MCR 302, Anton Paar Company (Graz, Austria). The sample used is subjected to a 20 mm diameter and 1 mm thickness, respectively. The sample was placed between a rotating disk and a parallel base plate (PP20/MRD/1T). An oscillatory shear test method was applied for all rheological tests, and the measuring temperature was kept constant at 25 °C. All sample were subjected to different magnetic field which are 0 T (off-state) and 0.8 T (on-state) as shown in Table 2. The strain amplitude sweep test was carried out by varying the strain from 0.0001% to 10% at constant frequency of 1 Hz. For the frequency sweep test, the frequency was swept from 0.1 to 100 Hz at a constant strain of 0.001% and for the magnetic field sweep test, the magnetic field was swept from 0 to 0.8 T at constant frequency (1 Hz) and strain (0.001%).

Table 2. Magnetic flux density.

Magnetic Flux Density (T)	Current (A)
0 T	0 A
0.8 T	5 A

For the resistance test, before it was carried out, the hardness of the samples was determined first by using elastomer shore A (HBA 100-0: Sauter GmbH, Balingen, German). The resistance of the MRE was observed using a test rig, as shown in Figure 2. It was set up to determine the resistance, from the exerted load applied between 1 to 5 kg in this experiment. The data acquisition (DAQ) used was obtained from LabVIEW (6211, National Instruments, Austin, TX, USA). After the connection was set up, the off-state test (without magnetic field) was conducted by placing a 1 kg weight on the MRE, and the load given was distributed equally on the entire surface of the tested sample. The test was then repeated until 5 kg at intervals of 1 kg. The on-state testing (with the magnetic field) was carried out in a similar condition, but the MRE was sandwiched between permanent magnets. These magnets were used to induce magnetic fields in the MRE in order to investigate the change in the resistance properties of the material.
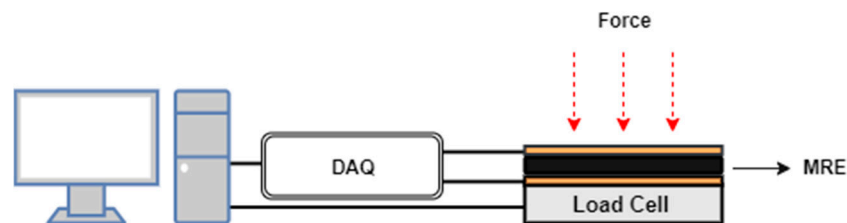
Figure 2. Schematic diagram for resistance testing.

3. Result and Discussion

3.1. Magnetic Properties

Figure 3 shows the hysteresis loops of the MRE sample that have been measured in the field up to 15,000 Oe. Magnetic saturation M_S, coercivity H_C, and retentivity magnetization, M_R were evaluated at room temperature. Table 3 shows the value on the magnetic behavior for the MRE. It can be easily comprehended that the cobalt particle exhibits ferromagnetic behavior as observed from the coercivity magnetic hysteresis. In addition, the two curves had similar magnetic saturation behaviors. The anisotropic MRE showed similar behavior regarding its hysteresis loop but with a higher magnetic saturation value compared to the isotropic MRE. The difference in magnetic performance of the MRE was mainly attributed to the particle alignment of the cobalt particle. This indicates that the alignment of particles in the anisotropic did influence the magnetic flux flow by causing stronger and closer inter-particle interaction. Thus, this kind of strong inter-particle interaction will result in higher magnetic saturation. As compared to the isotropic sample, random particle distribution caused the magnetic flux flow restricted by the silicon rubber.

Table 3. Magnetic properties of isotropic and anisotropic MRE.

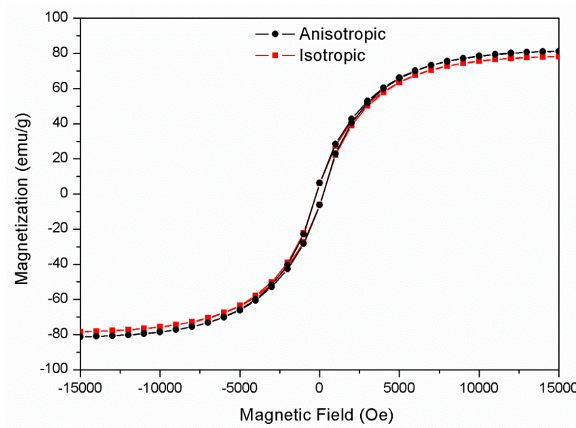| Sample	M_S, emu g^{-1}	M_r, emu g^{-1}	H_C, Oe
Isotropic	78.74	6.09	215.47
Anisotropic	81.29	6.34	216.97

Figure 3. Magnetic hysteresis loop of the Co-MRE.

3.2. Morphology of MRE

Isotropic and anisotropic MRE cross-section morphologies from the FESEM are shown in Figure 4. The cobalt particle had been observed to be embedded well and dispersed in the silicone rubber matrix. In Figure 4a, the particles show random distribution. This is because, during the preparation of MRE, there is no magnet existence that can cause the interaction between particles. In Figure 4b, the particles form a column structure. The magnetic field has been used during preparation, so the particles are magnetized and attracted to one another. The particles start to vibrate and shape the column structures after the magnetic force defeats the matrix resistance. Whereas, in the isotropic orientation they are randomly distributed because the particles are not affected by the direction of the magnetic field. The discussion of the impacts of structuring during preparation on the morphology will be followed in connection with the MR effect measured under a magnetic field.
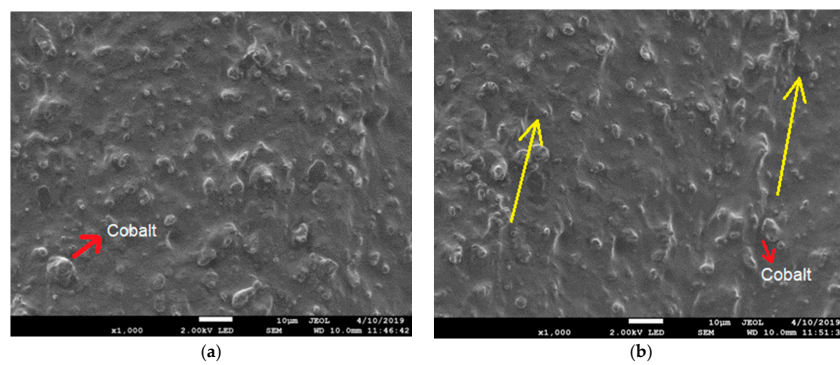

Figure 4. Field emission scanning electron microscopy (FESEM) images of (**a**) isotropic MRE and (**b**) anisotropic MRE with 53 wt % of cobalt.

Table 4 tabulated energy-dispersive X-ray spectroscopy (EDX) results obtained from the field emission scanning electron microscopy (FESEM) images. Based on the FESEM micrograph, several points were chosen to determine the composition of the elements in the MRE. Silicon exhibits the highest weight (41.66%) followed by cobalt and oxygen (31.37% and 26.97%). The element is present due to the use of silicone rubber as a matrix and cobalt as a magnetic particle in MRE fabrication.

Table 4. Elements percentage in the MRE.

Element	Weight (%)
Si	41.66
Co	31.37
O	26.97

4. Rheological Properties

4.1. Strain Amplitude Sweep Test

Figure 5 shows the storage modulus and loss factor of the MRE samples as a function of the strain amplitude under magnetic flux and constant frequency (1 Hz). The static oscillatory strain had been applied to the sample parallel with the particles alignment of anisotropic sample MRE. The strain amplitude depends on both the elastic and viscous behavior of the material. It can be observed that the storage and loss modulus had decreased with increasing strain amplitude for all sample. This phenomenon was strain-dependent behavior. Besides that, the strain amplitude had increased with magnetic field for all the samples. The anisotropic sample in on-state condition shows the highest storage and loss modulus values, which are 0.48 MPa and 0.038 Mpa. Meanwhile, isotropic MRE stated the lowest storage and loss modulus in an off-state condition, which is 0.25 Mpa and 0.017 Mpa. From the storage modulus, which was related to the stiffness behavior from the MRE point of view, the isotropic sample shows more stiffness than the anisotropic sample for both storage and loss modulus. The anisotropic stiffness sample is at 0.1% strain, while the isotropic sample is at 10% strain.
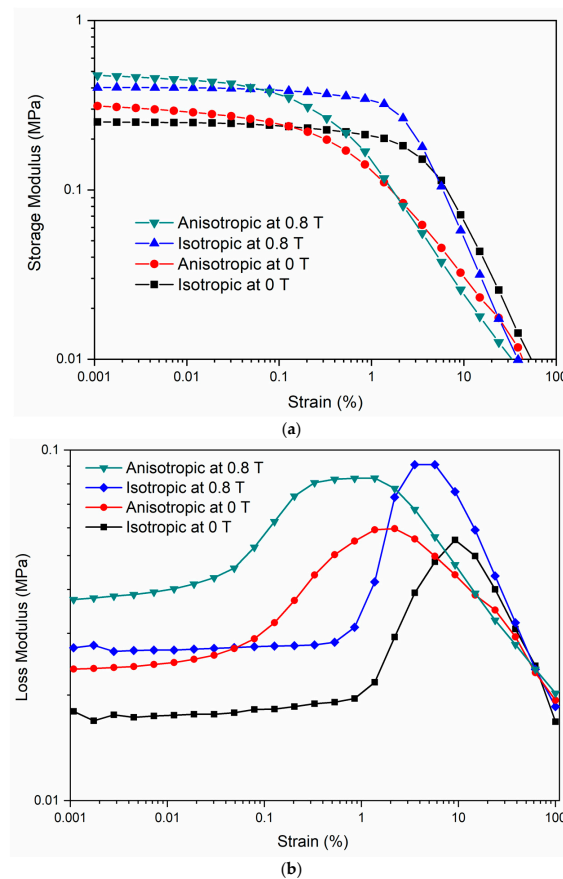

Figure 5. (**a**) Storage modulus and (**b**) loss modulus of MRE under different magnetic flux densities as a function of strain amplitude.

This phenomenon demonstrated a common payne effect behavior for MRE, where it indicates the reliance of storage modulus on strain amplitudes, which is caused by the devastation and restructuring of a cobalt particle bonding in the rubber [22]. The performance during the on-state condition, the Payne effect, had been more obvious. That is why the storage modulus of the on-state condition is higher than that of the off-state condition. In addition, the linear viscoelastic (LVE) region has a tendency to reduce by the external magnetic field. For the anisotropic sample, the application of a magnetic field of 0.8 T caused the particles that had been aligned to be repelled, which is why the anisotropic curve shows a

lower LVE as compared to the isotropic curve. When there is a higher magnetic field, the particle chain tended to be easily interrupted, which led to the shorter linear region of the MRE sample. The matrix is reinforced by the particles because of the physical interactions among the particles and the matrix, and subsequently, the LVE region is reduced [23]. The morphological properties are strongly supported, as observed in Table 4. Those chain structures were easily broken at higher strain during the oscillatory test due to the particles attracting edge to edge. Particle chains and the movement of the particles within the silicon rubber structure affect the loss modulus. To sum up, the storage and loss modulus increase with the increasing magnetic field strength can be attributed to the stronger network structure at a higher magnetic field. It indicates that both the anisotropic and isotropic curves present significant magnetorheological effects.

4.2. Frequency Sweep Test

Figure 6 shows the storage modulus and loss factor or tan δ of the MRE samples as a function of frequency. The storage and loss modulus for isotropic and anisotropic increased with the increasing frequency at the 0 and 0.8 T magnetic field. It is a typical phenomenon for viscoelastic material where frequency will cause an increase, since the deformation of the particle chain had been unsuccessful to sustain with the shear force in the matrix, thereby causing the storage modulus to increase with increasing frequency [24].
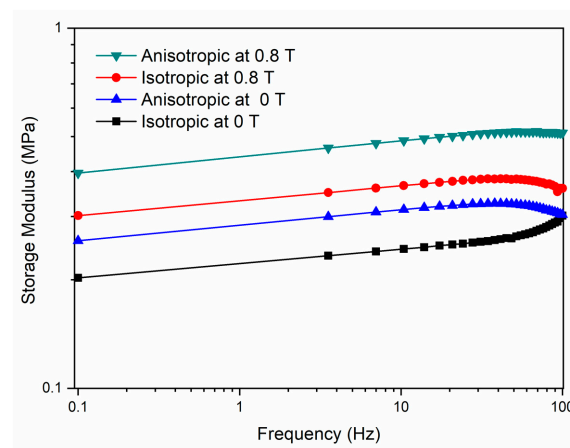
(**a**)
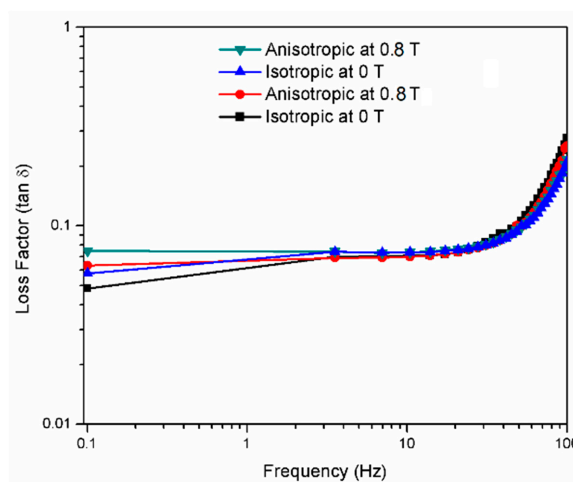
(**b**)

Figure 6. Storage modulus (**a**) and loss factor (**b**) of MRE under different magnetic flux densities as a function of frequency.

The storage modulus at an on-state condition was observed to be higher as compared to the off-state condition. Applying the magnetic field strengthened the interaction between the cobalt particles in the matrix. In addition, the magnetic field also led to stronger formation chains structures and will improve the storage modulus. The chain-like structure in the anisotropic MRE also causes the storage modulus of anisotropic MRE to be higher as compared to isotropic MRE. This is due to the easy magnetization axes between particles and led to a decrease of inter-particle distance.

Loss factor during the on-state condition for the isotropic and anisotropic samples had shown a higher value than during the off-state condition. A higher value of loss factor had higher heat dissipation, leading to stronger cobalt particle interaction. The lower value at the off-state condition for both the isotropic and anisotropic samples due to the smaller friction indirectly led to less energy dissipation [25]. On the other hand, a higher value of loss factor for the anisotropic sample indicates that the chain-like structure had turned out to be more complex and had reinforced the interaction force between the particle and the matrix [15]. Besides particle bonding, the interaction between the particle and matrix also influenced the value of the loss factor.

4.3. Magnetic Field Sweep Test

Figure 7 shows the storage modulus versus the magnetic field of the isotropic and anisotropic MRE at constant strain amplitude 0.001% and constant frequency of 1 Hz. As the magnetic field (T) increased, the storage modulus increased. It means that both isotropic and anisotropic MRE presents a typical MR effect, which can be attributed to the increasing magnetic attractive interaction between particles. Furthermore, the magnetic field would cause the cobalt particle to align and restrict the deformation of the matrix, therefore bringing about a change of the modulus. The MR effect can be expressed by the following equation:

$$G_{MRE}(\%) = \frac{\Delta G}{G_0} \times 100\%$$

where G_o is the initial storage modulus and ΔG is the difference between the maximum storage modulus and initial storage modulus and. The MR effect is presented in Table 5.
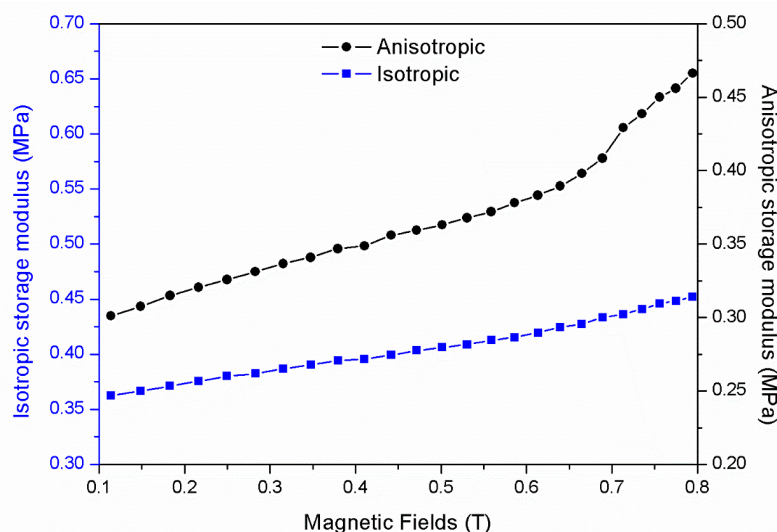

**Figure 7.** The MR effect of anisotropic and isotropic MRE at magnetic field of 0–0.8 T.

Table 5. The MR effect on the storage modulus of the MRE.

Sample	MR Effect (%)
Isotropic	27.77
Anisotropic	71.42

As shown in Table 5, the MR effect of anisotropic MRE is 61% higher than that of the isotropic MRE sample. Interaction between particles would become stronger under anisotropic conditions because of the chain-like structure formation during the curing process. In addition, the effect of the magnetic field will strengthen the attractive interaction between the particles in the anisotropic condition. Thus, this phenomenon explained the greater MR effect on the anisotropic MRE, which aligns with the previous study [26].

5. Resistance Properties

Compression test results for isotropic and anisotropic MRE under different applied forces and magnetic fields were initially obtained to evaluate the electrical resistivity of MRE, which explained the behaviour of the electric charge carrier in the MRE. Figure 8 shows the magnitude of resistance versus applied force for various magnetic fields. The hardness of the sample was Shore 57A for isotropic MRE and Shore 58A for anisotropic MRE. The experiment was conducted by applying a weight between 1 and 5 kg. The magnetic field also was varied between 0 T (off-state) and 0.1 T (on-state). It can be seen that the resistance was decreased exponentially as the weight changed by an increment of 1 kg for both the isotropic and anisotropic samples at off- and on-state conditions.
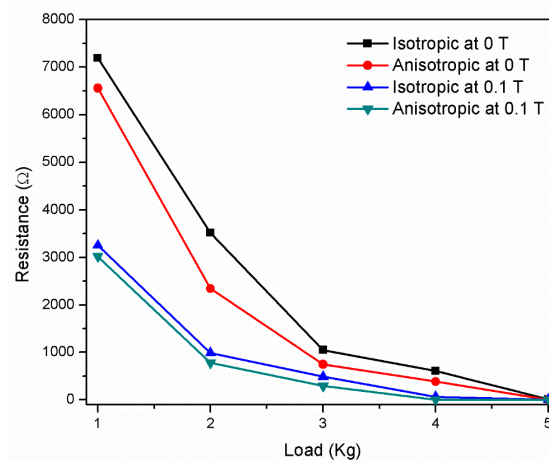
Figure 8. Resistance reduction of MRE in the magnetic field 0 (off-state) and 0.1 T (on-state).

By applying load to the MRE, the electrical resistance decreased for both the isotropic and anisotropic MRE. This can be referred to as the piezoresistance effect [27]. This phenomenon might be because the cobalt particle chains become closer between each particle. So, the decrease of the resistance will increase the electrical contact between the cobalt particles. The resistance of the anisotropic MRE is lower than that of the isotropic MRE. This is because the chain-like structure inside the MRE has made the electricity flow more efficiently. Indeed, the particle alignment also plays a big role in electric circulation in MRE. In addition, it can also be related to the MR effect, which shows that the anisotropic MRE has a higher MR effect than the isotropic sample. The higher modulus change can be attributed to the greater strength interaction between particles causing less resistance.

In addition, when applying a magnetic field to 0.1 T, the MRE results in a larger reduction in the resistance for both MRE. The magnetic field causes the cobalt particles instantaneously to become magnetic dipoles; they follow the direction of magnetic field lines, therefore forming a network of

parallel chains inside the MRE. By combining the applied force and magnetic field, the resistance of the MRE decreases with applied force.

The resistance changes at the very beginning, and gradually, the resistance reaches a nearly constant value. The correlation between magnetoresistance and piezoresistance in MRE is ascribable to the deformation of the material. This phenomenon also was discovered and consistent with the findings of Shabdin et al., who verified that by applying force and a magnetic field, the resistance would decrease [20].

6. Conclusions

In this study, cobalt-based MRE using silicon rubber was successfully fabricated in isotropic and anisotropic types. Besides the morphologies, element characterization, and magnetic properties, the relationship between rheological properties and magnetic field, the resistance, and magnetic field were also experimentally investigated and discussed in detail. Their microstructure was observed by FESEM and mapping analysis showing, the cobalt chain in an anisotropic state. Anisotropic MRE has shown higher magnetic saturation compared to isotropic MRE. A significant increment of the storage modulus of isotropic and anisotropic MRE was also observed under magnetic fields in strain and frequency sweep. Anisotropic MRE under a magnetic field exhibits the highest storage modulus for both sweep condition. An extraordinary MRE effect achieved by anisotropic MRE was 71.42%, which is 157% higher than that of isotropic MRE. Besides the magnetic properties, cobalt particles have generated conductivity to the MRE. The resistance was detected as the change in resistance, which is related to the external force generated from the contact to the MRE. This indicates that the controllable conductivity of MRE can be a potential candidate for wide application such as sensor applications. In a nutshell, the outcomes acquired from this study are seen as convenient and can be considered in the future studies of the MRE field.

References

1. Kumbhar, S.B.; Chavan, S.P.; Gawade, S.S. Adaptive tuned vibration absorber based on magnetorheological elastomer-shape memory alloy composite. *Mech. Syst. Signal Process.* **2018**, *100*, 208–223. [CrossRef]
2. Komatsuzaki, T.; Inoue, T.; TerasFighima, O. Mechatronics Broadband vibration control of a structure by using a magnetorheological elastomer-base d tune d dynamic absorb er. *Mechatronics* **2016**, *40*, 128–136. [CrossRef]
3. Sun, S.; Deng, H.; Yang, J.; Li, W.; Du, H. Performance evaluation and comparison of magnetorheological elastomer absorbers working in shear and squeeze modes. *J. Intell. Mater. Syst. Struct.* **2015**, *26*, 1757–1763. [CrossRef]
4. Moučka, R.; Goňa, S.; Sedlačík, M. Accurate measurement of the true plane-wave shielding effectiveness of thick polymer composite materials via rectangular waveguides. *Polymers* **2019**, *11*, 1603. [CrossRef] [PubMed]

5. Abramchuk, S.; Kramarenko, E.; Stepanov, G.; Nikitin, L.V.; Filipcsei, G. Novel highly elastic magnetic materials for dampers and seals: Part I. Preparation and characterization of the elastic materials. *Polym. Adv. Technol.* **2007**, *18*, 883–890. [CrossRef]

6. Liao, G.J.; Gong, X.; Xuan, S.H.; Kang, C.J.; Zong, L.H. Development of a real-time tunable stiffness and damping vibration isolator based on magnetorheological elastomer. *J. Intell. Mater. Syst. Struct.* **2011**, *23*, 25–33. [CrossRef]

7. Ausanio, G.; Iannotti, V.; Ricciardi, E.; Lanotte, L.; Lanotte, L. Physical Magneto-piezoresistance in Magnetorheological elastomers for magnetic induction gradient or position sensors. *Sens. Actuators A* **2014**, *205*, 235–239. [CrossRef]

8. Ge, L.; Gong, X.; Wang, Y.; Xuan, S. The conductive three dimensional topological structure enhanced magnetorheological elastomer towards a strain sensor. *Compos. Sci. Technol.* **2016**, *135*, 92–99. [CrossRef]

9. Volkova, T.I.; Böhm, V.; Kaufhold, T.; Popp, J.; Becker, F.; Borin, D.Y.; Stepanov, G.V.; Zimmermann, K. Motion behaviour of magneto-sensitive elastomers controlled by an external magnetic fi eld for sensor applications. *J. Magn. Magn. Mater.* **2017**, *431*, 262–265. [CrossRef]

10. Wan, Y.; Xiong, Y.; Zhang, S. Temperature dependent dynamic mechanical properties of Magnetorheological elastomers: Experiment and modeling. *Compos. Struct.* **2018**, *202*, 768–773. [CrossRef]

11. Qiao, X.; Lu, X.; Li, W.; Chen, J.; Gong, X. Microstructure and magnetorheological properties of the thermoplastic magnetorheological elastomer composites containing modified carbonyl iron particles and poly (styrene-b-ethylene-ethylenepropylene-b-styrene). *Smart Mater. Strucut.* **2012**, *21*, 115028. [CrossRef]

12. Landa, R.A.; Soledad Antonel, P.; Ruiz, M.M.; Perez, O.E.; Butera, A.; Jorge, G.; Oliveira, C.L.P.; Negri, R.M. Magnetic and elastic anisotropy in magnetorheological elastomers using nickel-based nanoparticles and nanochains. *J. Appl. Phys.* **2013**, *114*, 213912. [CrossRef]

13. Małecki, P.; Krolewicz, M.; Hiptmair, F.; Krzak, J.; Kaleta, J.; Major, Z.; Pigłowski, J. Influence of carbonyl iron particle coating with silica on the properties of magnetorheological elastomers. *Smart Mater. Struct.* **2016**, *25*, 105030. [CrossRef]

14. Lee, C.J.; Kwon, S.H.; Choi, H.J.; Chung, K.H.; Jung, J.H. Enhanced magnetorheological performance of carbonyl iron/natural rubber composite elastomer with gamma-ferrite additive. *Colloid Polym. Sci.* **2018**, *296*, 1609–1613. [CrossRef]

15. Jung, H.S.; Kwon, S.H.; Choi, H.J.; Jung, J.H.; Kim, Y.G. Magnetic carbonyl iron/natural rubber composite elastomer and its magnetorheology. *Compos. Struct.* **2016**, *136*, 106–112. [CrossRef]

16. Bica, I. Influence of the magnetic field on the electric conductivity of magnetorheological elastomers. *J. Ind. Eng. Chem.* **2010**, *16*, 359–363. [CrossRef]

17. Li, W.; Kostidis, K.; Zhang, X.; Zhou, Y. Development of a force sensor working with MR elastomers. In Proceedings of the 2009 IEEE/ASME International Conference on Advanced Intelligent Mechatronics, Singapore, 14–17 July 2009; pp. 233–238.

18. Tian, T.F.; Li, W.H.; Alici, G.; Du, H.; Deng, Y.M. Microstructure and magnetorheology of graphite-based MR elastomers. *Rheol. Acta* **2011**, *50*, 825–836. [CrossRef]

19. Schümann, M.; Morich, J.; Kaufhold, T.; Böhm, V.; Zimmermann, K.; Odenbach, S. A mechanical characterisation on multiple timescales of electroconductive magnetorheological elastomers. *J. Magn. Magn. Mater.* **2018**, *453*, 198–205. [CrossRef]

20. Shabdin, M.K.; Rahman, A.; Azizi, M.; Mazlan, S.A.; Hapipi, N.M.; Adiputra, D.; Aziz, S.A.A.; Bahiuddin, I.; Choi, S.B. Material Characterizations of Gr-Based Magnetorheological Elastomer for Possible Sensor Applications: Rheological and Resistivity Properties. *Materials* **2019**, *12*, 391. [CrossRef]

21. Tong, Y.; Dong, X.; Qi, M. Improved tunable range of the field-induced storage modulus by using flower-like particles as the active phase of magnetorheological elastomers. *Soft Matter* **2018**, *14*, 3504–3509. [CrossRef]

22. Sorokin, V.V.; Ecker, E.; Stepanov, G.V.; Shamonin, M.; Monkman, G.J.; Kramarenko, E.Y.; Khokhlov, A.R. Experimental study of the magnetic fi eld enhanced Payne e ff ect in magnetorheological elastomers. *Soft Matter* **2014**, *10*, 8765–8776. [CrossRef] [PubMed]

23. Phewthongin, N.; Saeoui, P.; Sirisinha, C. Rheological Behavior of CPE / NR Blends Filled with Precipitated Silica. *J. Appl. Polym. Sci.* **2006**, *100*, 2565–2571. [CrossRef]

24. Fan, Y.C.; Gong, X.L.; Jiang, W.Q.; Zhang, W.; Wei, B.; Li, W.H. Effect of maleic anhydride on the damping property of magnetorheological elastomers. *Smart Mater. Struct.* **2010**, *19*, 055015. [CrossRef]

25. Hapipi, N.; Aziz, S.A.A.; Mazlan, S.A.; Ubaidillah; Choi, S.B.; Mohamad, N.; Khairi, M.H.A.; Fatah, A.Y.A. The field-dependent rheological properties of plate-like carbonyl iron particle-based magnetorheological elastomers. *Results Phys.* **2019**, *12*, 2146–2154. [CrossRef]

26. Li, W.H.; Zhang, X.Z. A study of the magnetorheological effect of bimodal particle based magnetorheological elastomers. *Smart Mater. Strucut.* **2010**, *19*, 035002. [CrossRef]

27. Ghafoorianfar, N.; Wang, X.; Gordaninejad, F. Combined magnetic and mechanical sensing of magnetorheological elastomers. *Smart Mater. Strucut.* **2014**, *5*, 055010. [CrossRef]